

Biomechanical modeling of cancer - Agent-based force-based models of solid tumours within the context of the tumour microenvironment

Cicely Macnamara¹

¹University of St Andrews

January 30, 2024

Abstract

Once cancer is initiated, with normal cells mutated into malignant ones, a solid tumour grows, develops and spreads within its microenvironment invading the local tissue; the disease progresses and the cancer cells migrate around the body leading to metastasis, the formation of distant secondary tumours. Interactions between the tumour and its microenvironment drive this cascade of events which have devastating, if not fatal, consequences for the human host/patient. Among these interactions, biomechanical interactions are a vital component. In this paper, key biomechanical relationships are discussed through a review of modelling efforts by the mathematical and computational oncology community. The main focus is directed, naturally, towards lattice-free agent-based, force-based models of solid tumour growth and development. In such models interactions between pairs of cancer cells (as well as between cells and other structures of the tumour microenvironment) are governed by forces. These forces are ones of repulsion and adhesion, and are typically modelled via either an extended Hertz model of contact mechanics or using Johnson-Kendal-Roberts theory, both of which are discussed here. The role of the extracellular matrix in determining disease progression is outlined along with important cell-vessel interactions which combined together account for a great proportion of Hanahan and Weinberg's "Hallmarks of Cancer".

Biomechanical modelling of cancer: Agent-based force-based models of solid tumours within the context of the tumour microenvironment

Cicely K Macnamara^{a,*}

^a*School of Mathematics and Statistics, Mathematical Institute, University of St Andrews, United Kingdom, KY16 9SS*

Abstract

Once cancer is initiated, with normal cells mutated into malignant ones, a solid tumour grows, develops and spreads within its microenvironment invading the local tissue; the disease progresses and the cancer cells migrate around the body leading to metastasis, the formation of distant secondary tumours. Interactions between the tumour and its microenvironment drive this cascade of events which have devastating, if not fatal, consequences for the human host/patient. Among these interactions, biomechanical interactions are a vital component. In this paper, key biomechanical relationships are discussed through a review of modelling efforts by the mathematical and computational oncology community. The main focus is directed, naturally, towards lattice-free agent-based, force-based models of solid tumour growth and development. In such models interactions between pairs of cancer cells (as well as between cells and other structures of the tumour microenvironment) are governed by forces. These forces are ones of repulsion and adhesion, and are typically modelled via either an extended Hertz model of contact mechanics or using Johnson-Kendal-Roberts theory, both of which are discussed here. The role of the extracellular matrix in determining disease progression is outlined along with important cell-vessel interactions which combined together account for a great proportion of Hanahan and Weinberg's *Hallmarks of Cancer* [1, 2].

Keywords: agent-based; force-based; in silico tumours; cancer growth and development; tumour microenvironment

1. Introduction

2 The term cancer covers a spectrum of diseases – cancer cells can arise from
3 any type of cell in the body and can grow in or around any tissue or organ
4 making it highly complex. Tumour cells proliferate, occupying whole areas of

*Corresponding author

Email address: `ckm@st-andrews.ac.uk` (Cicely K Macnamara)

5 tissue; they interact with surrounding cells, tissue structures, vasculature and
6 the extracellular matrix (ECM) in a variety of ways. In recent years, mathem-
7 atical and computational biologists have endeavoured to accurately capture the
8 growth and development of tumours within their local environment through *in*
9 *silico* models. By simulating virtual tumours, insight is gleaned which comple-
10 ments traditional biological and experimental approaches to cancer research at
11 limited financial and ethical cost. This paper will focus on highlighting selec-
12 ted lattice-free agent-based (specifically force-based models) of tumour growth
13 and development. By way of introduction it will be worthwhile to discuss the
14 importance of approaching the problem from a mechanical standpoint, as such,
15 in Section 1.1, the tumour microenvironment (TM) is presented followed by, in
16 Section 1.2, a discussion of the inherent biomechanics of the TM. In Section 1.3
17 certain other modelling techniques which have been used to study the dynamics
18 of tumour growth and development will be highlighted paying specific attention
19 to where biomechanics have been successfully implemented.

20 1.1. The tumour microenvironment (TM)

21 The term *tumour microenvironment* is given to all aspects of the local en-
22 vironment of a tumour, consisting of, but not limited to, the surrounding blood
23 vessels/vasculature, ECM, tumour-associated immune cells and signalling mo-
24 lecules/proteins released by the cancer cells (see schematic in Figure 1). The
25 tumour and the TM are intrinsically linked and there is constant interplay and
26 interactions between them starting from the point of tumour initiation [3]. In-
27 deed, non-cancerous cells within tissue respond continuously to the external
28 signals of their environment, changing their metabolic state, growth, mitosis,
29 gene expression, differentiation, movement, or even undergoing programmed
30 cell death (apoptosis), accordingly. Should the cell fail to correctly transduce or
31 respond to a specific (external) signal it effectively becomes cancerous. A cell
32 with a cancerous phenotype has several distinct *Hallmarks* [1, 2]. For example,
33 cancer cells resist apoptosis and enable replicative immortality; this unchecked
34 proliferation creates a tumour (or neoplasm) within the tissue.

35 Tumours influence the TM in a variety of different ways. Hypoxic tumour
36 cells, starved of oxygen, are known to release vascular-endothelial growth factor
37 (VEGF) which promotes tumour angiogenesis, supplying the tumour with con-
38 stant access to vital nutrient [4, 5]. Equally, as the growing tumour vies for
39 space within the tissue, cells release matrix metalloproteinases (MMPs) which
40 degrade the ECM making room for tumour growth and local invasion [6, 7].
41 Conversely, the TM affects tumour growth and development; the shape and size
42 of a tumour; but also its genetic evolution being determined by properties of
43 the local environment. For example, cells migrate preferentially up gradients of
44 ECM stiffness in a specific type of mechanotaxis called *durotaxis* [8]. Stiff ECMs
45 can promote tumourigenesis through integrin-dependent mechanotransduction
46 at focal adhesions [9] while soft ECMs contribute to phenotypic selection of
47 tumour-repopulating cells (TRCs) [10]. Indeed the TM has been found to play
48 an active role in the progression of malignancies [11, 12].

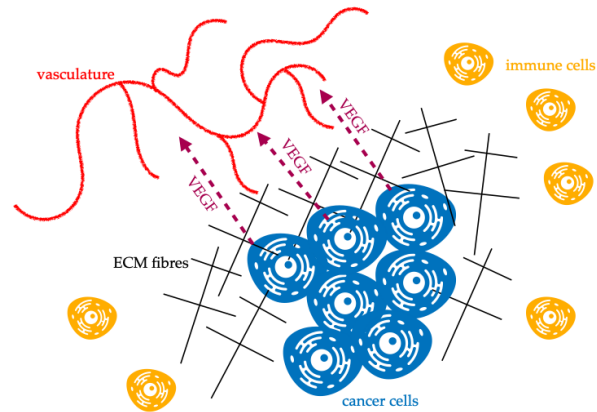


Figure 1: Schematic diagram showing several key aspects of the TM: the cancer cells (blue), the ECM fibres (black), the vasculature (red), vascular-endothelial growth factor (VEGF) signalling protein (magenta) and immune cells (orange).

49 One of the *Hallmarks of Cancer* is tissue invasion and metastasis in which
 50 tumours spread both locally and non-locally [1, 2]. Malignant tumours aggress-
 51 ively take over large areas of tissue, and, of greater concern, are able to move
 52 from primary locations to secondary locations using the body’s circulatory sys-
 53 tem. This is a major issue since it is commonly purported that as many as 90%
 54 of all cancer deaths are due to metastatic spread; note that this figure while
 55 widely reported and hypothesised is not yet scientifically proven although it is
 56 true that the majority of cancer fatalities are due to metastases [13]. Never-
 57 theless, agent-based models of tumours typically and vitally should also include
 58 aspects of the TM in order to model how cancers invade and metastasise.

59 *1.2. Biomechanics in the TM*

60 The focus of this paper is towards force-based models, and as such it is
 61 important to understand why mechanical interactions are so important. As
 62 discussed above there is constant interplay between a tumour and the TM.
 63 Indeed, the TM governs how a tumour establishes and develops; the tumour
 64 cells respond to mechanical cues actively by changing shape, state or migrating.
 65 For example, Friedl and co-workers have shown how the specific nature of the
 66 ECM (it’s density, stiffness and geometry) along with aspects of the cancer
 67 cell (it’s adhesive properties and polarity) determine how a cell (or a collection
 68 of cells) migrates through tissue [14–18]. *Durotaxis* was mentioned above but
 69 another type of “taxis” experienced by cells is *haptotaxis* [19] which is motility
 70 of cells preferentially up gradients of adhesion within the ECM. More generally
 71 cells are affected by “mechanotransduction”, in which cell-external mechanical
 72 stresses provoke cell-internal chemical signals leading to some type of adaptive
 73 response [20]. For further discussion of mechanotransduction in cancer see the

74 review of the same name [21]. Equally, within the tumour itself stresses affect
75 development. Homeostatic pressure in which a balance of proliferation and
76 apoptosis results in zero net growth has been found to limit the growth of some
77 solid tumours [22, 23]. Conversely, such mechanical compression (solid stress)
78 may actually drive cancer cells to invade and metastasise [24–27]. Given the
79 intrinsic links between cancer cell behaviour and biomechanics, in order to fully
80 understand how tumours, initiate, grow, invade and metastasise it is vital to
81 include such processes in mathematical and computational models.

82 *1.3. Other In Silico models*

83 Early mathematical modelling of cancer (avascular solid tumours) focused on
84 deterministic or continuum models of solid tumour spheroids developed from the
85 classical Greenspan model [28]. Such models continue to provide insight through
86 the ability to efficiently model large scale dynamics (typical palpable tumours
87 will contain at least 10^8 cells [29]) and equally since they lend themselves to
88 mathematical analysis. For reviews of deterministic and continuum models see,
89 for example, [30, 31]. Selected articles in which mechanical stress is modelled
90 using a continuum approach include [3, 32–36] while cell-cell interactions are
91 considered in [37–43], and cell-matrix interactions in [44].

92 More recently efforts have been focused on using individual-based models
93 or agent-based models which allow a more direct comparison to the biology
94 through the ability to model at the cell scale and within. In fact, modelling
95 cell behaviour on the individual level is naturally scale bridging allowing at
96 once intracellular (microscopic) and intercellular (mesoscopic) mechanisms to be
97 included even when modelling a large number of cells (macroscopic). Equally,
98 taking an individual approach easily allows the modelling of heterogenous cell
99 populations or, at the very least, variability between cells.

100 *1.3.1. On lattice models*

101 The most simplistic agent-based models are cellular automata models; in
102 general, on-lattice agent based models have dominated the literature, these can
103 be broadly categorised into four distinct types (see Table 1). Note, in the schem-
104 atics in Table 1 each type is shown on a structured square lattice, however, on-
105 lattice models often now use unstructured lattices such as the Voronoi-Delaunay
106 lattice, for example, which typically results in more biologically realistic shapes,
107 both of cells and cell-masses [46, 69]. On-lattice models may be 3D as in the case
108 of the classic multicellular tumour spheroid (MCTS) models or 2D as in the case
109 of monolayers. On-lattice models lend themselves to efficient large scale simu-
110 lations of a great number of cells at little computational cost. Table 1 provides
111 details of some selected references for state-of-the-art on-lattice models of tu-
112 mour growth, specifying the tumour-TM interactions considered where appro-
113 priate. For further discussion of on-lattice models see, for example, the reviews
114 in [69–75]. On-lattice models typically do not include mechanics which may be
115 necessary to accurately depict the biology (see discussion above). Types I, II
116 and IV rely solely on stochastic processes governing changes of state or position

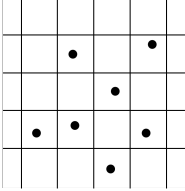
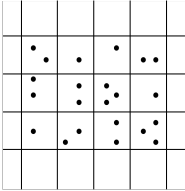
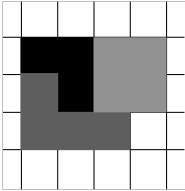
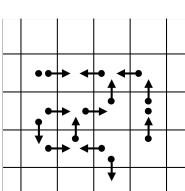
Schematic	Model Description	Selected References
	Type I - Single cell per lattice site	MCTS [45–47]; cell-vessel interactions [48]; cell adhesion [49–52]; monolayers [53]; phenotypic heterogeneity [54–57]
	Type II - Compartment model. Multiple cells per lattice site	coarse-grained proliferative rim [58, 59]
	Type III - Single cell covers multiple lattice sites (Cellular-Potts)	MCTS [60]; cell adhesion [61, 62]; angiogenesis [63]; cell-fibre interaction [64]; monolayers [65]
	Type IV - Multiple (or single) cell(s) per lattice site, movement through velocity channels (lattice gas cellular automata)	MCTS [66]; cell-fibre interaction [67]; cell-ECM interaction [68]

Table 1: Summary of on-lattice models with some selected references.

117 of a cell as well as mitosis. Cellular-Potts (Type III) is the only type to permit
118 the modelling of physical mechanisms by solving an effective energy equation
119 which goes some way to modelling the forces between cells (see, for example,
120 [76–78]). There are several open-source on-lattice computational frameworks
121 which include, notably for cancer, the *CompuCell3D* Cellular-Potts framework
122 [79].

123 The remainder of this paper considers lattice-free (or off-lattice) agent-based,
124 specifically, centre-based, force-based models of tumour growth and develop-
125 ment. It is structured as follows: in Section 2 the modelling approach is intro-
126 duced, in Section 3 the specifics of the forces acting between cells are outlined
127 and in Section 4 there is a discussion of selected modelling efforts of other as-
128 pects of the TM. Throughout, a sample of results from the literature will be
129 given.

130 **2. Centre-based force-based modelling**

131 Within a lattice-free agent-based model each component (e.g. cell, tissue
 132 fibre or vessel segment) is considered explicitly. Let us start by considering the
 133 most important aspect of the TM, the tumour cells themselves. Each cancer
 134 cell, i , is an individual agent; this paper focuses on centre-based models (CBM)
 135 in which the cell geometry is simplified with each cell considered to be a vis-
 136 coelastic sphere subject to small deformations, described by the position of its
 137 centre, \underline{x}_i , in the domain (hence centre-based) and its radius, R_i , see leftmost
 138 image of Figure 2. When growing tumours of significant size it is a reasonable
 139 assumption/simplification to make that cells may be represented by spheres.
 140 Other tumour models exist in which cells have non-spherical shape or are fully
 141 deformable, notably the work of Rejniak and coworkers [80–83]). However, these
 are not the subject of the review given here.

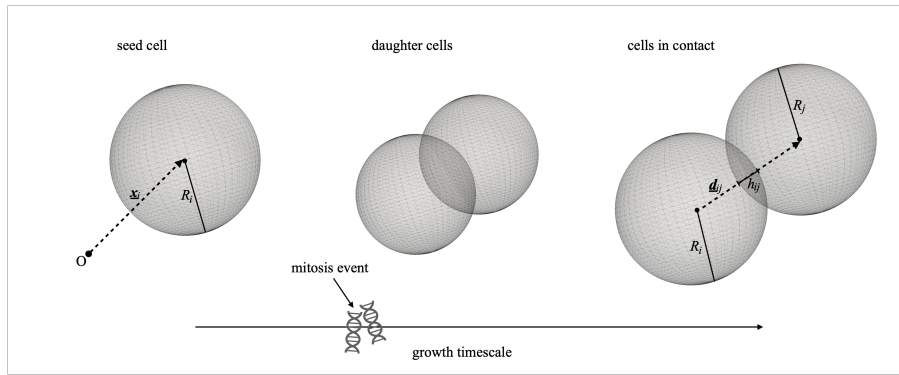


Figure 2: Schematic diagram indicating the basic physical properties of cells in centre-based models, showing on the left a single cell in isolation primed for mitosis, in the middle that seed cell having undergone mitosis creating two daughter cells and on the right two mature cells in contact under a balance of forces.

142 The behaviour of tumour cells can be broken down into three distinct but
 143 linked aspects. Firstly, there are biological factors such as the cell cycle; each cell
 144 has the ability to grow in size and divide, undergoing mitosis. Once a cell has
 145 reached maturity (proliferative size) it may split into two daughter cells; mitosis
 146 is considered a stochastic event (taking place randomly, indicated by the DNA
 147 segments on the growth timescale in Figure 2) with probability inverse to the
 148 cell-cycle time. When the mother cell divides the simplest implementation is
 149 to have two smaller (volume preserving) daughter cells replace the mother cell
 150 (see middle image of Figure 2) [84, 85], more sophisticated models depict the
 151 splitting more accurately by deforming the spherical mother cell into a dumbbell
 152 shape the ends of which eventually separate into the daughter cells [86, 87].
 153 The daughter cells then grow according to a growth rate until they too reach

155 proliferative size and experience forces imposed by each other (see below and
 156 Section 3). Mitosis may be inhibited by external factors such as an excessive
 157 compression force due to a high number of neighbouring cells, this is known as
 158 contact inhibition [86].

159 Secondly, there are genetic factors; cells may have given phenotypes or geno-
 160 types which prescribe their behaviour in some way. For example, cell phenotypic
 161 evolution might depend on biophysical processes, or biochemical interactions
 162 such as the availability of nutrients. This will be discussed further in Sec-
 163 tion 4.3.2, in which the traits of cells with a hypoxic phenotype are compared
 164 to the *Hallmarks of Cancer*.

165 Lastly, and particularly key, for force-based models interactions between cells
 166 (and indeed other agents in the model) are described by forces or potentials.
 167 Typically, each cell is governed by an equation of motion, an ordinary differential
 168 equation of the form:

$$\underbrace{\mathbf{\Gamma}\dot{\mathbf{x}}_i(t)}_{\text{friction}} + \underbrace{f_i(t)}_{\text{migration}} = \underbrace{\sum \mathbf{F}_i(t)}_{\text{mechanical forces}} . \quad (1)$$

169 The equation of motion takes into account three main aspects. Firstly, it ac-
 170 counts for friction experienced by the cell (first term in Equation (1), in which $\mathbf{\Gamma}$
 171 is a 3-dimensional tensor that models the physical structure of the environment)
 172 - this may be simply background friction imposed by the tissue but may account
 173 for friction imposed on cells by other structures. Secondly, the cell will have
 174 some pre-described active migration properties (second term in Equation (1)),
 175 these may be as simple as random fluctuations/motion as in [84, 85] or may
 176 take into account a cells preferred direction (polarity) as in [88] and even effects
 177 of the external environment (e.g. chemotaxis where cells are naturally driven
 178 up gradients of nutrient, as in [89]). Thirdly, it incorporates mechanical inter-
 179 actions via forces (third term in Equation (1)) between a cell and other agents
 180 within the model.

181 For two cells in contact (determined when the distance between their centres
 182 is less than the sum of their radii) a force directed along the vector between their
 183 centres, \mathbf{d}_{ij} , is calculated taking into account repulsion and adhesion. Resolving
 184 the resulting potential between the two cells in the absence of any migration
 185 terms leads to two cells which remain stationary under a balance of forces (see
 186 rightmost image of Figure 2). In the following Section we discuss in more
 187 detail the repulsion and adhesion forces between cells. Later we will outline
 188 interactions of cells with other aspects of the TM (Section 4).

189 3. Repulsion and Adhesion Forces

190 Force-based models are naturally governed by forces, specifically, repulsion
 191 and adhesion forces. In this Section the repulsion and adhesion forces acting
 192 between cancer cells are elucidated. The types of model discussed assume that
 193 a cell is spherical in isolation. Thus, any large contact area between a pair
 194 of cells (and indeed multiple contact areas between a cell and multiple others)

195 creates a significant stress on the cytoskeleton of the cell(s). The limited ability
 196 to deform or indeed compress (with Poisson numbers found by experiments to
 197 be between approximately 0.4 – 0.5 [90]) leads to repulsion between cells. Con-
 198 versely, cells are naturally adhesive. For cells in contact, binding due to adhesive
 199 molecules occurs; as the contact area increases so too do the adhesive bonds.
 200 The adhesive molecules at play are Cadherins (calcium-dependent adhesion)
 201 and Catenins, together these proteins form complexes called adherens junctions
 202 which facilitate cell-cell adhesion. Ramis-Conde and coauthors incorporated the
 203 E-Cadherin- β -Catenin pathway explicitly into their individual based model of
 204 tumour development in order to discuss the implications of this pathway on cell
 205 migration and cancer invasion [91–94].

206 The total cell-cell interaction force between two cells, i and j , directed along
 207 the vector, \mathbf{d}_{ij} , joining their centres (see righthmost image of Figure 2), is given
 208 by

$$\mathbf{F}_{i,j} = (\mathbf{F}_{i,j}^{\text{rep}} - \mathbf{F}_{i,j}^{\text{adh}}) \frac{\mathbf{d}_{ij}}{\|\mathbf{d}_{ij}\|}, \quad (2)$$

209 where $\mathbf{F}_{i,j}^{\text{rep}}$ is the repulsion force discussed in Section 3.1 and $\mathbf{F}_{i,j}^{\text{adh}}$ is the adhesion
 210 force discussed in Section 3.2. In order to calculate the change in position of
 211 cell i at each timestep, the sum of all resulting forces between cell i and any cell
 212 j with which it is in contact is included in the equation of motion (Equation 1).

213 3.1. Hertzian Repulsion

214 For two spherical cells, i and j , in contact and subject to small (elastic)
 215 deformations, the repulsive force experienced is typically described in the liter-
 216 ature by the classical Hertzian contact mechanics repulsion [95]. The form of
 217 the repulsion force for two such cells of radii R_i and R_j , is, therefore

$$|\mathbf{F}_{i,j}^{\text{rep}}| = \frac{4}{3} E^* R^{*1/2} h_{ij}^{3/2}, \quad (3)$$

218 where $h_{ij} = R_i + R_j - \|\mathbf{d}_{ij}\|$ describes the length of “overlap” (or contact area)
 219 between the two cells. This repulsion force term includes both an effective
 220 radius, $R^* = R_i R_j / (R_i + R_j)$ and an effective Young’s Modulus, E^* , which is
 221 calculated from

$$\frac{1}{E^*} = \frac{1 - \nu_i^2}{E_i} + \frac{1 - \nu_j^2}{E_j}, \quad (4)$$

222 where E_i and E_j are the cells’ respective Young’s moduli and ν_i and ν_j their
 223 Poisson ratios.

224 Under Hertzian elastic contact alone the following assumptions must be
 225 made: (a) strains on the cells are small and within the elastic limit, (b) the
 226 area of contact between the spherical cells is much smaller than their radii, (c)
 227 the cell surfaces are continuous and non-conforming and (d) there is no friction
 228 between the cells. Moreover, this classical model is strictly non-adhesive. Cells,
 229 however, are naturally adhesive, governed by adhesion molecules that travel

230 to the cellular membrane, stimulated by the proximity of a neighbouring cell,
 231 forming adhesive bonds. Thus, for those modelling mechanical cell-cell interac-
 232 tions using contact mechanics it is necessary to also include an adhesion force
 233 between cells, thus extending or modifying the classical Hertzian model.

234 3.2. Adhesion

235 There are several examples in the literature of cell-cell interaction forces,
 236 with differing expressions for the adhesive force, $\mathbf{F}_{i,j}^{\text{adh}}$. Here we discuss two key
 237 variants. These are outlined in Table 2 for quick reference and comparison.
 238 In each case the force takes into account the strength of adhesion, α , which is
 239 assumed to be constant among the cell population and considers the contact
 240 surface area between cells since as contact surface area increases so too does the
 number of adhesive bonds.

Adhesive Force	Description	References
$ \mathbf{F}_{i,j}^{\text{adh}} = \alpha S_{ij}$, e.g. $= 2\pi\alpha \left(R_i - \frac{h_{ij}}{4} \right) h_{ij}$	Adhesion directly propor- tional to contact surface area, S_{ij} . The resulting force can be determined explicitly.	[84, 85, 91, 92, 96]
$ \mathbf{F}_{i,j}^{\text{adh}} = \frac{4E^*}{3R^*} a^3 - [8\pi\alpha E^* a^3]^{1/2}$	Johnson-Kendal-Roberts (JKR) theory. Contact surface area (with contact radius parameter a) is modified by adhesion. The resulting force must be determined implicitly.	[87, 97, 98]

Table 2: Selected forms of CBM adhesion force with selected references.

241

242 3.2.1. Explicit adhesion force

243 In this variant, the adhesion force, $\mathbf{F}_{i,j}^{\text{adh}}$, between two overlapping cells, is
 244 assumed be directly proportional to the contact surface between them, S_{ij} .
 245 The contact surface area is first calculated which then feeds into the adhesion
 246 force. Within the literature there are different approximations for the contact
 247 surface area. In [96], for example, they model the contact surface area of cells in
 248 contact as the area of the circle equidistant between the two cells, underlying the
 249 spherical cap of height $h_{ij}/2$ (i.e. half the overlap between cells). While in [84]
 250 they calculate the area to be the average value between the area of the spherical
 251 cap of height the overlap between the cells, h_{ij} , and area of the circle underlying
 252 the cap (see Figure 3). In this case, the contact surface is approximated as

$$S_{ij} = \frac{1}{2} [2\pi R_i h_{ij} + \pi (2R_i h_{ij} - h_{ij}^2)] = 2\pi R_i h_{ij} + \frac{\pi h_{ij}^2}{2},$$

253 with the resulting adhesion force given by

$$|\mathbf{F}_{i,j}^{\text{adh}}| = 2\pi\alpha \left(R_i - \frac{h_{ij}}{4} \right) h_{ij}. \quad (5)$$

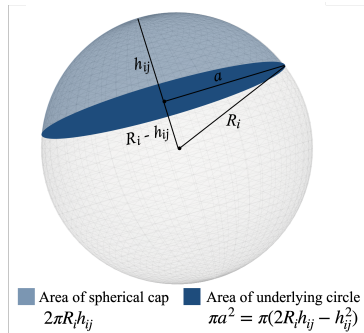


Figure 3: Figure showing how the contact area is estimated in [84].

254

255

256

257

258

259

260

261

262

263

This approach to modelling adhesion considers a “suction” effect as a consequence of the increasing density of effective bonds between the cells. In such an approach certain assumptions have been made [96]. Firstly, it is assumed that the adhesion molecules (receptors and ligands) which bind the cells together are distributed homogeneously over the whole cell surface and thus the whole contact surface area. Secondly, that binding takes place instantaneously and furthermore that since adhesion which causes deformations to the cell naturally change the cell surface area it is assumed that this process happens rapidly so that it is not necessary to explicitly consider the cell surface area.

264

265

266

267

Figure 4 shows the growth of a MCTS over 3 000 time steps (approximately 2 days) in which adhesion is modelled by the explicit adhesion force given by Equation 5. The simulation results shown are derived from the model (along with parameters) given in [85].

268

269

270

271

272

273

274

3.2.2. Implicit JKR adhesion force

The explicit model(s) of adhesion discussed in the previous Section, do not take into account the fact that the adhesion (derived from the surface contact area) then affects and modifies the surface contact area. The Johnson-Kendall-Roberts (JKR) theory of adhesive contact derives a model for the adhesive force which includes this hysteresis phenomena [99]. In this case the force is given by

$$|\mathbf{F}_{i,j}^{\text{adh}}| = \frac{4E^*}{3R^*} a^3 - [8\pi\alpha E^* a^3]^{1/2}, \quad (6)$$

275

276

in which E^* and R^* are, once again, the effective Young’s modulus and radius, respectively and a is the contact surface radius (see Figure 3). However, in this

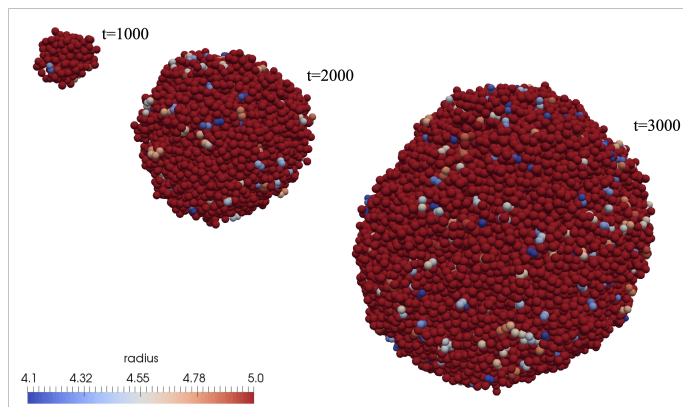


Figure 4: Figures showing the results of a computational simulation of the growth over time of a MCTS from the CBM of [85] (unpublished result) in which adhesion is incorporated via Equation 5.

277 case a is not fixed but rather changes and may be calculated from

$$h_{ij} = \frac{a^2}{R^*} - \left[\frac{2\pi\alpha a}{E^*} \right]^{1/2}. \quad (7)$$

278 Figure 5 is reproduced, with permission, from [98] (their Figure 5) in which
 279 they directly compare the behaviour of cells governed by (A) an explicit extended
 280 Hertzian model of adhesion (Section 3.2.1) with (B) the JKR theory model
 281 (Section 3.2.2). This study of the destabilisation of a monolayer shows clearly
 282 how the hysteresis effect between attachment and detachment of cells within
 283 the JKR model leads to fewer cells detaching from the substrate over the same
 284 timescale when compared with the extended Hertz model. For further details
 285 of the model parameters in these simulations, see [98].

286 For more details and simulation results of tumour growth under either the
 287 modified Hertzian or JKR adhesion forces see, for example, the references in
 288 Table 2.

289 4. Additional aspects of the TM

290 This review will now consider selected modelling efforts of the mathematical
 291 and computational oncology community with regards to modelling tumour-TM
 292 interactions. In Section 4.1 cell-ECM interactions are discussed while in Sec-
 293 tion 4.3 cell-vessel interactions are considered.

294 4.1. Tumour interactions with the ECM

295 The ECM, on a basic level, is composed of a structured mesh (matrix) of
 296 fibres (e.g. collagen and fibronectin) within a gel of glycoproteins. We have

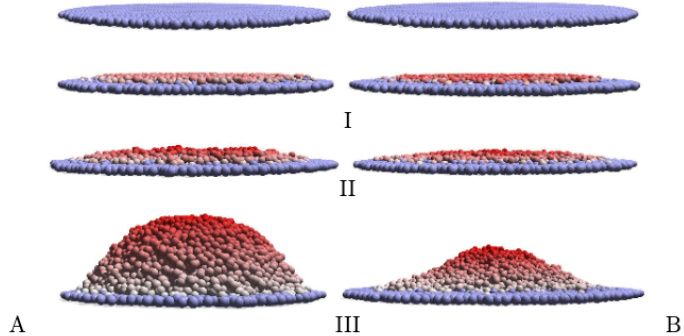


Figure 5: Destabilization of a monolayer using the extended Hertz interaction (A) and the JKR-interaction energy (B). The numbers (I), (II), (III) denote the knocked-out control mechanisms which lead the destabilisation. (I) contact inhibition, (II) anchorage-dependent proliferation (III) anchorage-dependent apoptosis (anoikis). PERMISSION PENDING

297 previously discussed cell-cell adhesion but another important adhesive process
 298 in cell biology is cell-matrix adhesion. Focal adhesions are protein complexes
 299 which connect the cell’s cytoskeleton to the ECM [9, 100]. Focal adhesions
 300 not only directly and mechanically link the cell to the ECM but they also act
 301 as points of signalling (mechanotransduction); transmitting information about
 302 the mechanics of the extracellular environment to cells through biochemical sig-
 303 nalling molecules. Focal adhesion mechanotransduction plays an important role
 304 in regulating both the shape and migration of cells [9]. Specific focal adhesion
 305 proteins which act as mechanotransducers are the ECM protein, fibronectin,
 306 and cell-membrane receptor integrins. Fibronectin also binds to collagen fibres
 307 in the ECM. Collagen fibres give structure to tissue but also, naturally, by
 308 extension, to the TM.

309 The fibrous connective tissue of the ECM performs a wide variety of functions
 310 within the healthy body. In terms of cancer, and within the TM, the structure of
 311 the ECM and the interaction of cancer cells with individual fibres of the matrix
 312 drives both cell proliferation and migration. ECM binding is implicated, for
 313 example, in proliferative signalling; experimental data, backed up by *in silico*
 314 models, have shown that border cells (those connected to the ECM) of a MCTS
 315 are less proliferative than cells in the interior [46]. Moreover, malignant cells
 316 activate the “integrin migration pathway” and crawl towards and along the
 317 protein network of the ECM; migration through the protein network results
 318 in the rearrangement of the ECM structure as cancer cells use the integrin
 319 pathway to cut-off the fibres and re-orient the ECM [101, 102]. Cell migration
 320 can happen as a collective process that presents in different ways depending
 321 on the tumour type and the nearby environment leading to different migration
 322 structures [15, 17]. The physical properties of the environment itself affects

323 tumour development and progression. It is widely known that cells prefer stiff
324 matrices to softer ones (*durotaxis*, [8]). Tumours themselves are known to be
325 stiffer than normal tissue [103]. Furthermore, it has been shown that stiff ECM
326 promotes tumour progression [104, 105]. On the other hand it has been shown
327 that tumour-repopulating cells (TRCs) are more proliferative in soft rather than
328 stiff environments [10]. To fully understand cancer development and local tissue
329 invasion it is important to model the ECM alongside the cancer cells. To model
330 the ECM it is natural to incorporate fibres as additional agents within an agent-
331 based model.

332 4.2. Cell-fibre interactions

333 In [88] the ECM fibres are modelled using a force-based, individual-based
334 model. Single-cell experiments are carried out to determine the affect that the
335 cell’s environment (in this case a 2D substrate) has on its migration. By placing
336 a single cell in a domain segregated by substrates with different matrix stiff-
337 nesses [88] were able to reproduce the experimental results of [8] showing that
338 cells are drawn preferentially to stiffer matrices, hypothesising that it was the
339 lack of matrix reorientation by the cell that drives *durotaxis*. In a second ex-
340 periment they showed the observable “follow-the-leader” behaviour of collective
341 cell migration [106]. Figure 6 reproduces, with permission, their Figure 10, in
342 which a single non-polarised cell becomes polarised and “follows” the path of
343 polarised “leader” cell.

344 In [85] the 2D model of [88] is extended to 3D and matrix fibres are in-
345 corporated into a CBM for tumour growth. Each individual fibre is modelled
346 explicitly by a thin cylinder (described by its extrema and radius), and the
347 three-dimensional computational domain is filled with fibres of a given distri-
348 bution of positions and orientations. In a similar way to cell-cell interactions,
349 cell-fibre interactions are governed by attractive and repulsive forces; a cell in
350 contact with a fibre will feel an adhesive force, parallel to fibre orientation and
351 a repulsive force orthogonal to the fibre [107]. The cell-fibre interaction force is
352 computed as the sum of these orthogonal/repulsive and parallel/adhesive terms,
353 $\mathbf{F}_{i,f} = F_{\parallel} - F_{\perp}$. The combined force $\mathbf{F}_{i,f}$ is added to the right-hand side of the
354 equation of motion of each cell (Equation 1). We outline the chosen forms of
355 the forces given in [85] in the following Section.

356 4.2.1. Cell-fibre forces

357 The cell-fibre adhesive force between a cell, i , and fibre, f , is modelled in
358 [85] by

$$\mathbf{F}_{\parallel} = \alpha_{\text{fibre}} \left(1 - \frac{\|\mathbf{v}_i\|}{v_{\text{max}}}\right) \left(\frac{|\mathbf{v}_i \cdot \mathbf{l}_f|}{\|\mathbf{v}_i\|}\right)^s \mathbf{l}_f. \quad (8)$$

359 It is directed along the normalised direction vector the fibre, \mathbf{l}_f , and depends on
360 the normalised scalar product between fibre direction and cell velocity (polarity),
361 $\mathbf{v}_i \cdot (\hat{\mathbf{x}}_i)$. Thus, this force is maximised when a cell is already travelling parallel
362 to the fibre in question. Moreover, the force depends on an adhesion coefficient,
363 α_{fibre} , and on a threshold velocity, v_{max} , which limits the pulling effect of fibres.

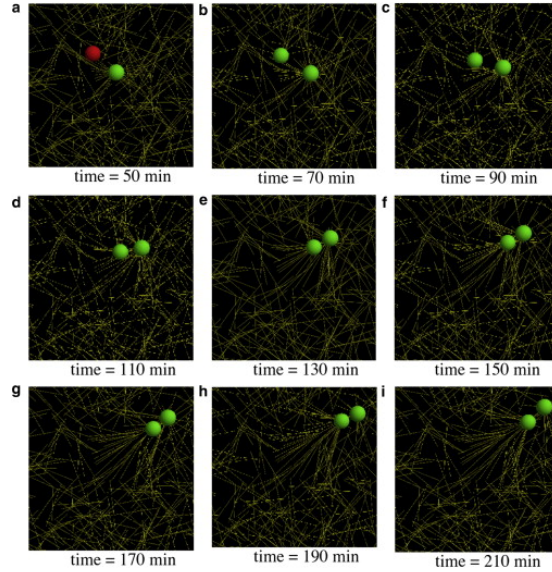


Figure 6: Snapshots in time indicating how two cells collectively migrate through the matrix. A non-polarized cell (red in plot **a**) becomes polarized (turning green) and then follows the path of the existing polarized cell (green in plot **a**). Reprinted from [88], Copyright (2012), with permission from Elsevier.

364 The additional parameter $s > 0$ is used to model additional effects which might
 365 increase ($s < 1$) or decrease ($s > 1$) the pulling effect.

366 The cell-fibre repulsion force is modelled via an additional friction exerted
 367 by the fibre, given in [85] by

$$\mathbf{F}_{\perp} = \beta_{\text{fibre}} \left(\frac{\|\mathbf{v}_i\|^2 - |\mathbf{v}_i \cdot \mathbf{l}_f|^2}{\|\mathbf{v}_i\|^2} \right)^r \mathbf{v}_i. \quad (9)$$

368 It is directed parallel to cell velocity and depends on the component of cell
 369 velocity orthogonal to the fibre, being maximised when the cell is travelling
 370 directly orthogonal to the fibre in question. The coefficient of cell-fibre friction
 371 is β_{fibre} and the exponent $r > 0$ can be used to model nonlinear effects which
 372 increase ($r < 1$) or decrease ($r > 1$) the repulsive forces.

373 Figure 7 is reproduced, with permission, from [85] (their Figure 4) shows how
 374 a tumour develops oriented along fibres which are uniformly distributed aligned
 375 with the y -axis. Initially a single cancer cell is placed within a fibrous domain,
 376 the resulting tumour which has developed (after 9 000 timesteps, approximately
 377 6 days) is shown in Figure 7. Whereas, in the absence of fibres, one would
 378 typically see a spherical tumour mass form (as in Figure 4), here the growth
 379 has been stretched out along the fibrous tissue. For further details of the model
 380 and associated parameters, see [85].

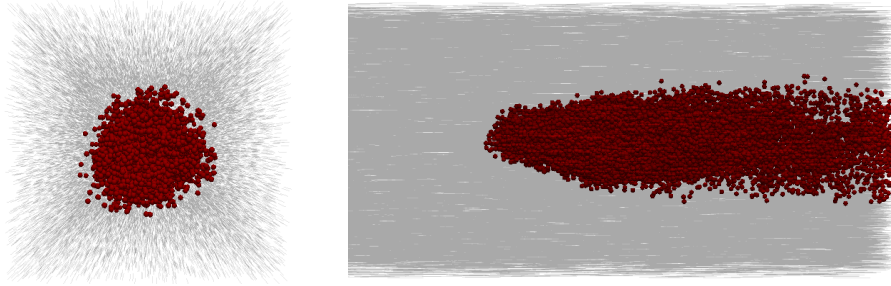


Figure 7: Figures showing the results of a simulation of tumour growth within a domain of uniformly distributed fibres (aligned with the y -axis) after 9 000 time steps. Cells are represented by red spheres, fibres in grey. Left: View orthogonal to the fibre orientation (xz -plane). Right: View in the yz -plane, cropped on the left side. Reprinted from [85], Copyright (2020), with permission from Elsevier.

381 Figure 8 (simulated under the model of [85]) shows the migration of a single
 382 (non-proliferating) cell within a given fibrous domain. On the lefthand of the
 383 domain fibres are directed at 45 degrees to the x -axis while they are aligned
 384 parallel to the x -axis on the righthand of the domain. The cell is placed at
 385 (250,50,250) shown by the blue circle. The simulation is run 50 times for
 386 10 000 timesteps (approximately 7 days), while the path of the cell through the
 387 fibrous domain is monitored. The trajectories of the cell for each simulation
 388 are indicated by the light grey lines, with the final position marked in red. The
 389 mean path is indicated with the dark grey line. As can be seen the cell paths
 390 follow the orientation of the fibres, switching alignment as they cross from the
 391 left to righthand of the domain.

392 A further biologically relevant aspect that links cancer cells to the ECM
 393 is matrix re-modelling. Matrix metalloproteinases (MMPs) are enzymes which
 394 degrade ECM proteins (e.g. collagen fibres) through proteolysis. Proteolytic
 395 re-modelling of the ECM by MMPs is a key step towards cancer invasion [6].
 396 Fibre degradation is taken into account in current state-of-the-art continuum
 397 models, see, for example, [108]. Alternative models of cell-ECM interactions
 398 include [109] who use Hookean springs which act via the basement membrane
 399 which links cells to the connective tissue.

400 4.3. Tumour interactions with the Vasculature

401 Another important aspect of the TM is the vasculature. Blood vessels weave
 402 through the tissue supplying it with oxygen and other vital nutrients. Cell-vessel
 403 interactions are both mechanical and biochemical.

404 4.3.1. Mechanical cell-vessel interactions

405 Cells interact mechanically with segments of the vessel network. In [85]
 406 they assume that repulsive and adhesive forces act between a cell and a vessel

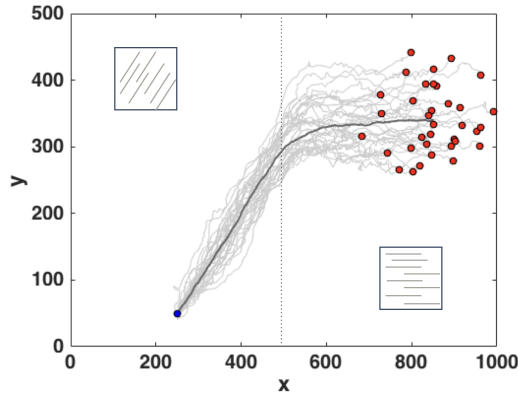


Figure 8: Cell migration simulation within a segregated domain of distributed fibres (not shown) after 10 000 time steps. The distribution of the fibres is indicated by the cartoons, being different on the lefthand and righthand sides. The initial position of the cell is indicated by the blue circle and the final positions (of 50 simulations) by red circles with paths shown in light grey. The average path is depicted in dark grey. Unpublished result from [85].

407 segment and that these forces are analogous to those between cells (Section 3),
 408 for further details see [85]. Their simulations show tumours developing and
 409 embedding within pre-existing vasculature. The proliferation of cancer cells
 410 around blood vessels - modelling so called “tumour cords” is simulated in [89].
 411 In the case of a tumour chord rather than a spherical tumour growing with the
 412 classical radial profile (necrotic core, quiescent and proliferative outer ring) the
 413 opposite profile is derived with necrotic regions on the outside furthest away
 414 from the central blood vessel(s). Figure 9 is reproduced, with permission, from
 415 [89] (their Figure 15).

416 In order for cancer to metastasise and spread to secondary sites around the
 417 body, cancer cells must be able to access the vessel network. Intravasation (and
 418 its analogous reverse, extravasation) is the process by which a cell enters (or
 419 leaves) the vascular network. In [92] they model the key metastatic process of
 420 intravasation using a CBM coupled to a deterministic model of the intracellular
 421 protein pathways which allow cells to migrate through the vessel endothelial
 422 wall (transendothelial migration, TEM) [110, 111]. In this case adhesion of the
 423 cancer cell with the vessel endothelia is key, and as before adhesion is driven by
 424 cadherins. Vascular endothelial cadherins (VE-cadherin) bind the cells of the
 425 vessel wall together. A cancer cell disrupts endothelial bonds binding itself to
 426 the wall using N-cadherin. Figure 10 is reproduced, with permission, from [92]
 427 and shows a single cell approach and then intravasate a vessel wall.

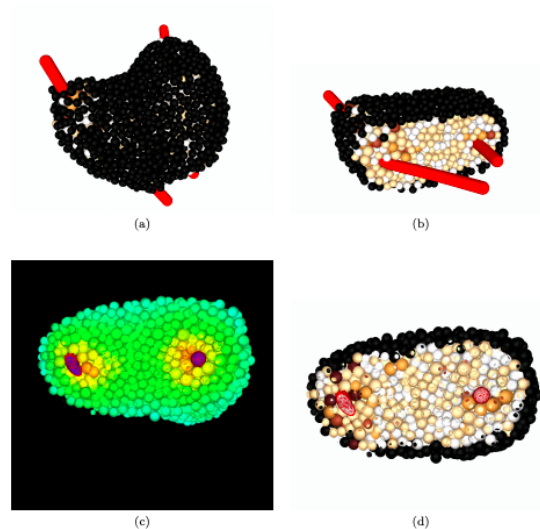


Figure 9: Simulation results of a tumour cord interacting with two blood vessels (black cells are necrotic). (a-b) Tumour cord growing around two vessels, (c) oxygen profile levels in the tumour cord, (d) cross-section showing corresponding development of tumour cells. Reprinted by permission from Springer Nature Customer Service Centre GmbH: Springer Nature, *Bulletin of Mathematical Biology*, [89], COPYRIGHT (2018).

428 *4.3.2. Biochemical interactions - The hypoxic phenotype*

429 Cancer cells, like normal cells, respond to the availability of oxygen, although
 430 the malignant response is anything but normal. We can characterise cancer
 431 cells into phenotypes based on their access to oxygen (e.g. normoxic, hypoxic
 432 and necrotic). Hypoxic cells are chronically lacking in sufficient oxygen, this
 433 deficiency of the main cell nutrient rather than being tumour suppressing actually
 434 drives tumour progression in numerous ways [5]. Jain lists the following
 435 responses of tumour cells to hypoxia: switch to anaerobic metabolism; resist ap-
 436 optosis; undergo the epithelial-mesenchymal transition (EMT); induce a cancer
 437 stem-cell “repopulating” phenotype, resist anti-cancer therapies; cause inflam-
 438 mation and immunosuppression; genomic instability and angiogenic. Notice
 439 that these classical behaviours are closely aligned with the *Hallmarks of Cancer*
 440 [1, 2]; the hypoxic phenotype is what drives cancer progression and makes it so
 441 deadly.

442 Hypoxia is a main driver of the epithelial-mesenchymal transition (EMT)
 443 [112]. The EMT occurs when epithelial cells detach (losing their cell-cell ad-
 444 hesion and polarity) and gain mesenchymal cell attributes (migration, invasion
 445 and differentiation). The EMT is the first step towards cancer metastasis. In
 446 [113] they model the EMT and metastasis using a hybrid on-lattice individual

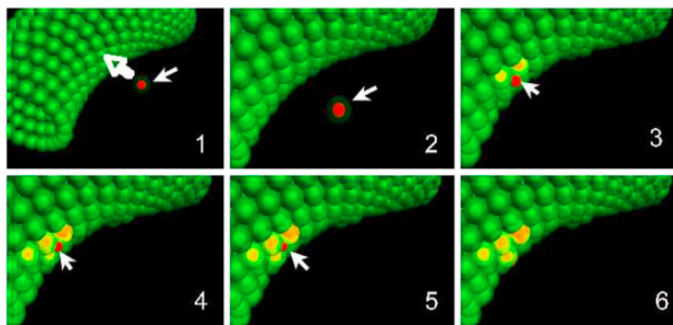


Figure 10: Spatio-temporal evolution dynamics of a malignant cell (red nucleus coloured cell, marked with a full arrow) approaching a blood vessel to undergo TEM. When the malignant cell attaches to the vessel, the VE-cadherin bonds are disrupted and new N-cadherin bonds are formed (shown in yellow). After some time, the malignant cell manages to disrupt the endothelial bonds enough to open a gap in the vessel and undergo TEM. Reproduced with permission from [92]. PERMISSION PENDING.

447 based approach. Hypoxia also drives angiogenesis, with hypoxic tumour cells
 448 releasing vascular-endothelial growth factor (VEGF) which signals for tumour
 449 angiogenesis. McDougall and coworkers are leading experts in modelling an-
 450 giogenesis [114–118]. In [84] they incorporate normoxic, hypoxic and necrotic
 451 phenotypes into a CBM to show how the hypoxia phenotype is implicated in the
 452 formation of pseudopalisades (hypercellular “walls” surrounding necrotic zones)
 453 in glioblastoma.

454 5. Conclusions

455 This paper provides a selective review of *in silico* models for tumour growth
 456 and development, with specific emphasis on centre-based force-based agent
 457 based models. Key authors in the field include Drasdo and coworkers [86, 97,
 458 98, 119–121] while a great many other authors are contributing to this vibrant
 459 area of research [84, 85, 122–126]. For a critical evaluation of the available
 460 agent based modelling techniques, their advantages and disadvantages see, for
 461 example, [69]. No review of such models would be complete without mentioning
 462 the work of Macklin and co-authors [127–129] who have recently launched *Physi-*
 463 *Cell* a comprehensive open source C++ code designed to simulate the growth
 464 of tumours within the TM [130]. One aspect of the TM which has not been
 465 discussed here, although which is a vital part, are tumour-associated immune
 466 cells. *PhysiCell* has been used to model how immune cells attack a MCTS [130],
 467 other agent-based models of tumour immune interactions-include [131–134].

468 The main take home message is that biomechanics need to be taken into
 469 account. One might contrast individual-based models with reaction-diffusion

470 models of cancer. While reaction-diffusion models (for example, [135–137])
471 do offer insight they do not include biomechanics nor can they account for
472 phenotypic variations that are well captured through an agent-based force-
473 based approach. Even for the subset of reaction-diffusion-taxis models ([138],
474 for example) where biomechanics may be implied they are not taken into ac-
475 count explicitly. Individual-based modelling, then, has significant advantages
476 over reaction-diffusion models in determining the key mechanisms which drive
477 metastatic spread. Perhaps in the future effort should be put into integrating
478 reaction-diffusion models with biomechanics in order to gain the advantages of
479 both approaches.

480 Agent-based modelling of tumour growth, however, is just a single strategy
481 in the global effort of the scientific community in the fight against cancer. Indeed
482 mathematical (and computational) oncology is a growing field in which research
483 is being done on a broad range of topics spanning from modelling intracellular
484 genetic pathways (see, for example, [139–141]) to modelling cancer therapies
485 (see, for example, [142–144]). Looking to the future a multi-scale model of
486 a growing tumour within the TM should seek to bring together not only the
487 biomechanical aspects laid out above but equally other aspects from the diverse
488 field of study. By incorporating intracellular pathways (such as in [91, 93]) which
489 results in phenotypic differences between cells it is possible to derive a realistic
490 heterogeneous cancer cell population. By using imaging combined with the
491 modelling techniques above to render *in vivo* tumours *in silico* it is possible to
492 simulate in real time and space the development of tumours predicting how they
493 will invade and metastasise. By trialing cancer therapies on *in silico* tumours
494 (as in [47, 118, 145]) clinicians can devise optimal therapy protocols that can
495 at once become both the standard of care and patient specific. In combination
496 these techniques will truly push the frontier of our understanding of cancer
497 and lead towards personalised medicine where each patient can be treated truly
498 individually.

499 Acknowledgements

500 CKM gratefully acknowledges the support of EPSRC Grant No.
501 EP/N014642/1 (EPSRC Centre for Multiscale Soft Tissue Mechanics - With
502 Application to Heart & Cancer).

503 References

- 504 [1] D. Hanahan and R. A. Weinberg. Hallmarks of cancer. Cell, 100:57–70,
505 2000.
- 506 [2] D. Hanahan and R. A. Weinberg. Hallmarks of cancer: the next genera-
507 tion. Cell, 144:646–674, 2011.
- 508 [3] Y. Kim, M. A. Stolarska, and H. G. Othmer. The role of the microenviron-
509 ment in tumor growth and invasion. Prog Biophys Mol Biol, 106:353–379,
510 2011.

- 511 [4] G. D. Yancopoulos, S. Davis, N. W. Gale, J. S. Rudge, S. J. Wiegand,
512 and J. Holash. Vascular-specific growth factors and blood vessel formation.
513 Nature, 407(6801):242–248, 2000.
- 514 [5] R. K. Jain. Antiangiogenesis strategies revisited: from starving tumors to
515 alleviating hypoxia. Cancer Cell, 26(5):605–622, 2014.
- 516 [6] L. M. Coussens and Z. Werb. Matrix metalloproteinases and the develop-
517 ment of cancer. Chem Biol, 3(11):895–904, 1996.
- 518 [7] Y. Itoh and H. Nagase. Matrix metalloproteinases in cancer. Essays
519 Biochem, 38:21–36, 2000.
- 520 [8] C.-M. Lo, H.-B. Wang, M. Dembo, and Y.-L. Wang. Cell movement is
521 guided by the rigidity of the substrate. Biophys J, 79(1):144–152, 2000.
- 522 [9] J. Seong, N. Wang, and Y. Wang. Mechanotransduction at focal adhe-
523 sions: from physiology to cancer development. J Cell Mol Med, 17(5):597–
524 604, 2013.
- 525 [10] J. Liu, Y. Tan, H. Zhang, Y. Zhang, P. Xu, J. Chen, Y. C. Poh, K. Tang,
526 N. Wang, and B. Huang. Soft fibrin gels promote selection and growth of
527 tumorigenic cells. Nat Mater, 11(8):734–741, 2012.
- 528 [11] T. Brabletz, A. Jung, S. Reu, M. Porzner, F. Hlubek, L. A. Kunz-
529 Schughart, R. Knuechel, and T. Kirchner. Variable beta-catenin expres-
530 sion in colorectal cancers indicates tumor progression driven by the tumor
531 environment. Proc Natl Acad Sci USA, 98:10356–10361, 2001.
- 532 [12] T. Brabletz, S. Spaderna, J. Kolb, F. Hlubek, G. Faller, C. J. Bruns,
533 A. Jung, J. Nentwich, I. Duluc, C. Domon-Dell, T. Kirchner, and J. N.
534 Freund. Down-regulation of the homeodomain factor cdx2 in colorectal
535 cancer by collagen type i: an active role for the tumor environment in
536 malignant tumor progression. Cancer Res, 64:6973–6977, 2004.
- 537 [13] H. Dillekås, M. S. Rogers, and O. Straume. Are 90% of deaths from cancer
538 caused by metastases? Cancer Med, 8:5574–5576, 2019.
- 539 [14] P. Friedl, K. S. Zänker, and E-B. Bröcker. Cell migration strategies in 3-d
540 extracellular matrix: Differences in morphology, cell matrix interactions,
541 and integrin function. Microsc Res Tech, 43:369–378, 1998.
- 542 [15] P. Fiedl and K. Wolf. Tumour-cell invasion and migration: diversity and
543 escape mechanisms. Nat Rev Cancer, 3(5):362–374, 2003.
- 544 [16] K. Wolf, Y. I. Wu, Y. Liu, J. Geiger, E. Tam, C. Overall, M. S. Stack, and
545 P. Friedl. Multi-step pericellular proteolysis controls the transition from
546 individual to collective cancer cell invasion. Nat Cell Biol, 9(8):893–904,
547 2007.

- 548 [17] P. Fiedl and K. Wolf. Proteolytic interstitial cell migration: a five-step
549 process. Cancer Metastasis Rev, 28(1-2):129–135, 2009.
- 550 [18] P. Fiedl and S. Alexander. Cancer invasion and the microenvironment:
551 plasticity and reciprocity. Cell, 147(5):992–1009, 2011.
- 552 [19] J. A. Davies, editor. Chapter 11 - Guidance by Contact, pages 129–145.
553 Academic Press, 2013.
- 554 [20] T. Iskratsch, H. Wolfenson, and M. P. Sheetz. Appreciating force and
555 shape the rise of mechanotransduction in cell biology. Nat Rev Mol Cell
556 Biol, 15:825–833, 2014.
- 557 [21] L. Chin, Y. Xia, D. E. Discher, and P. A. Janmey. Mechanotransduction
558 in cancer. Curr Opin Chem Eng, 11:77–84, 2016.
- 559 [22] G. Helmlinger, P. A. Netti, H. C. Lichtenbeld, R. J. Melder, and R. K.
560 Jain. Solid stress inhibits the growth of multicellular tumor spheroids.
561 Nat Biotechnol, 15:778–783, 1997.
- 562 [23] G. Cheng, J. Tse, R. K. Jain, and L. L. Munn. Micro-environmental mech-
563 anical stress controls tumor spheroid size and morphology by suppressing
564 proliferation and inducing apoptosis in cancer cells. PLoS ONE, 4:e4632,
565 2009.
- 566 [24] J. Yang, S. A. Mani, J. L. Donaher, S. Ramaswamy, C. Itzykson, R.
567 A. Come, P. Savagner, I. Gitelman, A. Richardson, and Weinberg R. A.
568 Twist, a master regulator of morphogenesis, plays an essential role in
569 tumor metastasis. Cell, 117(7):927–939, 2004.
- 570 [25] M. Basan, T. Risler, J. F. Joanny, X. S. Garau, and J. Prost. Homeostatic
571 competition drives tumor growth and metastasis nucleation. HFSP J,
572 3(4):265–272, 2009.
- 573 [26] D. T. Butcher, T. Alliston, and V. M. Weaver. A tense situation: Forcing
574 tumour progression. Nat Rev Cancer, 9:108–122, 2009.
- 575 [27] J. M. Tse, G. Cheng, J. A. Tyrrell, S. A. Wilcox-Adelman, Y. Boucher,
576 R. K. Jain, and L. L. Munn. Mechanical compression drives cancer cells
577 toward invasive phenotype. PNAS, 109(3):911–916, 2012.
- 578 [28] H. P. Greenspan. Models for the growth of a solid tumour by diffusion.
579 Stud Appl Math, 52:317–340, 1972.
- 580 [29] U. Del Monte. Does the cell number 10(9) still really fit one gram of tumor
581 tissue? Cell Cycle, 8(3):505–506, 2009.
- 582 [30] R. P. Araujo and McElwain D. L. S. A history of the study of solid
583 tumour growth: the contribution of mathematical modelling. Bull Math
584 Biol, 66(5):1039–1091, 2004.

- 585 [31] T. Roose, S. J. Chapman, and P. K. Maini. Mathematical models of
586 avascular tumor growth. SIAM Rev, 49(2):179–208, 2007.
- 587 [32] A. F. Jones, H. M. Byrne, J. S. Gibson, and J. W. Dold. A mathematical
588 model of the stress induced during avascular tumour growth. J Math Bio,
589 40(6):473–499, 2000.
- 590 [33] D. Ambrosi and F. Mollica. On the mechanics of a growing tumor. Int J
591 Eng Sci, 40(12):1297–1316, 2002.
- 592 [34] C. Koike, T. D. McKee, A. Pluen, S. Ramanujan, K. Burton, L. L. Munn,
593 Y. Boucher, and R. K. Jain. Solid stress facilitates spheroid formation:
594 potential involvement of hyaluronan. Br J Cancer, 86:947–953, 2002.
- 595 [35] H. Byrne and L. Preziosi. Modelling solid tumour growth using the theory
596 of mixtures. Math Med Biol, 20:341–366, 2003.
- 597 [36] D. Ambrosi and F. Mollica. The role of stress in the growth of a multicell
598 spheroid. J Math Biol, 48(5):477–479, 2004.
- 599 [37] H. Byrne and M. A. J. Chaplain. Modelling the role of cell-cell adhesion
600 in the growth and development of carcinomas. Math Comput Model,
601 12:1–17, 1996.
- 602 [38] H. Byrne. The importance of intercellular adhesion in the development of
603 carcinomas. IMA J Math Appl Med Biol, 14:305–323, 1997.
- 604 [39] C. Breward, H. Byrne, and C. Lewis. The role of cell-cell interactions in a
605 two-phase model for avascular tumour growth. J Math Biol, 45:125–152,
606 2002.
- 607 [40] H. M. Byrne, J. R. King, D. L. S. McElwain, and L. Preziosi. A two-phase
608 model of solid tumor growth. Appl Math Lett, 16(4):567–573, 2003.
- 609 [41] N. J. Armstrong, K. J. Painter, and J. A. Sherratt. A continuum approach
610 to modelling cell-cell adhesion. J Theor Biol, 243:98–113, 2006.
- 611 [42] M. A. J. Chaplain, L. Graziano, and L. Preziosi. Mathematical modelling
612 of the loss of tissue compression responsiveness and its role in solid tumour
613 development. Math Med Biol, 23:197–229, 2006.
- 614 [43] I. Ramis-Conde, M. A. J. Chaplain, and A. Anderson. Mathematical
615 modelling of cancer cell invasion of tissue. Math Comput Model, 47:533–
616 545, 2008.
- 617 [44] L. Preziosi and A. Tosin. Multiphase modeling of tumor growth and
618 extracellular matrix interaction: mathematical tools and applications. J
619 Math Biol, 58(4-5):625–656, 2008.

- 620 [45] A. R. Kansal, S. Torquato, G. R. IV Harsh, E. A. Chiocca, and T. S. Deis-
621 boeck. Simulated brain tumor growth dynamics using a three dimensional
622 cellular automaton. J Theor Biol, 203(4):367–382, 2000.
- 623 [46] N. Jagiella, B. Müller, M. Müller, I. E. Vignon-Clementel, and D. Drasdo.
624 Inferring growth control mechanisms in growing multi-cellular spheroids
625 of nslc cells from spatial-temporal image data. PLoS Comput Biol,
626 12(2):e1004412, 2016.
- 627 [47] S. C. Brüningk, P. Ziegenhein, I. Rivens, U. Oelfke, and G. T. Haar. A
628 cellular automaton model for spheroid response to radiation and hyper-
629 thermia treatments. Sci Rep, 9(1):17674, 2019.
- 630 [48] A. A. Patel, E. T. Gawlinski, S. K. Lemieux, and R. A. Gatenby. A
631 cellular automaton model of early tumor growth and invasion: The effects
632 of native tissue vascularity and increased anaerobic tumor metabolism. J
633 Theor Biol, 213(3):315–331, 2001.
- 634 [49] A. R. A. Anderson. A hybrid model of solid tumour invasion: the import-
635 ance of cell adhesion. Math Med Biol, 22:163186, 2006.
- 636 [50] A. R. A. Anderson, A. M. Weaver, P. T. Cummings, and V. Quaranta.
637 Tumor morphology and phenotypic evolution driven by selective pressure
638 from the microenvironment. Cell, 17(5):905–915, 2006.
- 639 [51] M. Aubert, M. Badoual, S. Freol, C. Christov, and B. Grammaticos. A
640 cellular automaton model for the migration of glioma cells. Phys Biol,
641 3:93–100, 2006.
- 642 [52] J. Vivas, D. Garzón-Alvarado, and M. Cerrolaza. Modeling cell adhesion
643 and proliferation: a cellular-automata based approach. Adv Model Simul
644 Eng Sci, 2:32, 2015.
- 645 [53] M. Block, E. Schöll, and D. Drasdo. Classifying the expansion kinetics
646 and critical surface dynamics of growing cell populations. Phys Rev Lett,
647 99(24):248101, 2007.
- 648 [54] A. R. A. Anderson, K. A. Rejniak, P. Gerlee, and V. Quaranta. Modelling
649 of cancer growth, evolution and invasion: Bridging scales and models.
650 Math Model Nat Phenom, 2(3):1–29, 2007.
- 651 [55] L. Zhang, C. G. Strouthos, Z. Wang, and T. S. Deisboeck. Simulating
652 brain tumor heterogeneity with a multiscale agent-based model: Link-
653 ing molecular signatures, phenotypes and expansion rate. Math Comput
654 Model, 49(1-2):307–319, 2009.
- 655 [56] H. Enderling and P. Hahnfeldt. Cancer stem cells in solid tumors: Is ‘evad-
656 ing apoptosis’ a hallmark of cancer? Prog Biophys Mol Biol, 106(2):391–
657 399, 2011.

- 658 [57] Y. Cai, J. Wu, S. Xu, and Z. Li. A hybrid cellular automata model of
659 multicellular tumour spheroid growth in hypoxic microenvironment. J
660 Appl Math, 2013:519895, 2013.
- 661 [58] M. Radszuweit, M. Block, J. Hengstler, E. Schöll, and D. Drasdo. Com-
662 paring the growth kinetics of cell populations in two and three dimensions.
663 Phys Rev E, 79:051907, 2009.
- 664 [59] D. Chen, Y. Jiao, and S. Torquato. A cellular automaton model for tumor
665 dormancy: emergence of a proliferative switch. PloS one, 9(10):e109934,
666 2014.
- 667 [60] E. Stott, N. Britton, J. Glazier, and M. Zajac. Stochastic simulation of
668 benign avascular tumor growth using the potts model. Math Comput
669 Model, 30:183–198, 1999.
- 670 [61] S. Turner and J.A. Sherratt. Intercellular adhesion and cancer invasion: a
671 discrete simulation using the extended potts model. J Theor Biol, 216:85–
672 100, 2002.
- 673 [62] E. Boghaert, D. C. Radisky, and C. M. Nelson. Lattice-based model of
674 ductal carcinoma in situ suggests rules for breast cancer progression to an
675 invasive state. PLoS Comput Biol, 10:e1003997, 2014.
- 676 [63] A. Shirinifard, J. S. Gens, B. L. Zaitlen, N. J. Popawski, M. Swat, and
677 J. A. Glazier. 3d multi-cell simulation of tumor growth and angiogenesis.
678 PLoS ONE, 4(10):e7190, 2009.
- 679 [64] B. M. Rubenstein and L. J. Kaufman. The role of extracellular matrix
680 in glioma invasion: a cellular potts model approach. Biophys J, 95:5661–
681 5680, 2008.
- 682 [65] J. F. Li and J. Lowengrub. The effects of cell compressibility, motility and
683 contact inhibition on the growth of tumor cell clusters using the cellular
684 potts model. J Theor Biol, 343:79–91, 2014.
- 685 [66] S. Dormann and A. Deutsch. Modeling of self-organized avascular tumor
686 growth with a hybrid cellular automaton. In Silico Biol, 2:393–406, 2002.
- 687 [67] M. Wurzel, C. Schaller, M. Simon, and A. Deutsch. Cancer cell invasion
688 of normal brain tissue: Guided by prepattern? J Theor Med, 6(1):21–31,
689 2005.
- 690 [68] H. Hatzikirou and A. Deutsch. Cellular automata as microscopic models of
691 cell migration in heterogeneous environments. Curr Top Dev Biol, 81:401–
692 434, 2008.
- 693 [69] P. Van Liedekerke, M. M. Palm, N. Jagiella, and D. Drasdo. Simulating
694 tissue mechanics with agent-based models: concepts, perspectives and
695 some novel results. Comp Part Mech, 2:401–444, 2015.

- 696 [70] J. Moreira and A. Deutsch. Cellular automaton models of tumor devel-
697 opment: a critical review. Adv Complex Syst, 5:247–268, 2002.
- 698 [71] M. S. Alber, M. A. Kiskowski, J. A. Glazier, and Y. Jiang. On cellu-
699 lar automaton approaches to modeling biological cells. In J. Rosenthal
700 and D. S. Gilliam, editors, Mathematical systems theory in biology,
701 communication, and finance, pages 1–39. The IMA Volumes in Math-
702 ematics and its Applications, vol 134. Springer, New York, NY, 2003.
- 703 [72] A. R. A. Anderson, M. A. J. Chaplain, and K. A. Rejniak.
704 Single-cell-based models in biology and medicine. Birkhäuser, Basel, 2007.
- 705 [73] A. Szabó and R. M. H. Merks. Cellular potts modeling of tumor growth,
706 tumor invasion and tumor evolution. Front Oncol, 3:87, 2013.
- 707 [74] H. Hatzikirou, G. Breier, and A. Deutsch. Cellular automaton modeling
708 of tumor invasion. In R. Meyers, editor, Encyclopedia of Complexity and
709 Systems Science, pages 1–13. Springer, Berlin, Heidelberg, 2014.
- 710 [75] J. Metzcar, Y. Wang, R. Heiland, and P. Macklin. A review of cell-based
711 computational modeling in cancer biology. JCO Clin Cancer Inform, 3:1–
712 13, 2019.
- 713 [76] N. Ouchi, J. A. Glazier, J. Rieu, A. Upadhyaya, and Y. Sawada. Improving
714 the realism of the cellular potts model in simulations of biological cells.
715 Physica A, 329(3-4):451–458, 2003.
- 716 [77] M. Scianna and L. Preziosi. A hybrid model describing different morpho-
717 logies of tumor invasion fronts. Math Model Nat Phenom, 7(1):78–104,
718 2012.
- 719 [78] J. T. Daub and R. M. H. Merks. A cell-based model of extracellularmatrix-
720 guided endothelial cell migration during angiogenesis. Bull Math Biol,
721 75(8):1377–1399, 2013.
- 722 [79] M. H. Swat, G. L. Thomas, J. M. Belmonte, A. Shirinifard, D. Hmeljak,
723 and J. A. Glazier. Chapter 13 - multi-scale modeling of tissues using
724 compuCell3d. In A. R. Asthagiri and A. P. Arkin, editors, Computational
725 Methods in Cell Biology, volume 110 of Methods in Cell Biology, pages
726 325–366. Academic Press, 2012.
- 727 [80] K. A. Rejniak. A single-cell approach in modeling the dynamics of tumor
728 microregions. Math Biosci Eng, 2:643–655, 2005.
- 729 [81] K. A. Rejniak. An immersed boundary framework for modelling the
730 growth of individual cells: an application to the early tumour develop-
731 ment. J Theor Biol, 247:186–204, 2007.
- 732 [82] K. A. Rejniak and R. H. Dillon. Aa single cell-based model of the ductal
733 tumour microarchitecture. Comput Math Methods Med, 8(1):51–69, 2007.

- 734 [83] K. A. Rejniak, S. E. Wang, N. S. Bryce, H. Chang, B. Parvin, J. Jour-
735 quin, L. Estrada, J. W. Gray, C. L. Arteaga, A. M. Weaver, V. Quar-
736 anta, and A. R. A. Anderson. Linking changes in epithelial morphogenesis
737 to cancer mutations using computational modeling. PLoS Comput Biol,
738 6(8):e1000900, 2010.
- 739 [84] A. Caiazzo and I. Ramis-Conde. Multiscale modelling of palisade forma-
740 tion in glioblastoma multiforme. J Theor Biol, 383:145–156, 2015.
- 741 [85] C. K. Macnamara, A. Caiazzo, I. Ramis-Conde, and M. A. J. Chaplain.
742 Computational modelling and simulation of cancer growth and migration
743 within a 3d heterogeneous tissue: the effects of fibre and vascular struc-
744 ture. J Comp Sci, 40:101067, 2020.
- 745 [86] D. Drasdo and S. Hoehme. Individual-based approaches to birth and death
746 in avascular tumors. Math Comput Model, 37:1163–1175, 2003.
- 747 [87] H. Byrne and D. Drasdo. Individual-based and continuum models of grow-
748 ing cell populations: a comparison. J Math Biol, 58(657):301–313, 2009.
- 749 [88] D. K. Schlüter, I. Ramis-Conde, and M. A. J. Chaplain. Computational
750 modeling of single-cell migration: the leading role of extracellular matrix
751 fibers. Biophys J, 103:1141–1151, 2012.
- 752 [89] Z. Szymańska, M. Cytowski, E. Mitchell, C. K. Macnamara, and M. A. J.
753 Chaplain. Computational modelling of cancer development and growth:
754 Modelling at multiple scales and multiscale modelling. Bull Math Biol,
755 80:1366–1403, 2018.
- 756 [90] R. E. Mahaffy, S. Park, E. Gerde, J. Käs, and C. K. Shih. Quantitative
757 analysis of the viscoelastic properties of thin regions of fibroblasts using
758 atomic force microscopy. Biophys J, 86(3):1777–1793, 2004.
- 759 [91] I. Ramis-Conde, D. Drasdo, A. R. A. Anderson, and M. A. J. Chaplain.
760 Modeling the influence of the e-cadherin-beta-catenin pathway in cancer
761 cell invasion: a multiscale approach. Biophys J, 95(1):155–65, 2008.
- 762 [92] I. Ramis-Conde, M. A. J. Chaplain, A. R. A. Anderson, and D. Drasdo.
763 Multi-scale modelling of cancer cell intravasation: the role of cadherins in
764 metastasis. Phys Biol, 6(1):016008, 2009.
- 765 [93] I. Ramis-Conde and D. Drasdo. From genotypes to phenotypes: classifica-
766 tion of the tumour profiles for different variants of the cadherin adhesion
767 pathway. Phys Biol, 9(3):036008, 2012.
- 768 [94] D. K. Schlüter, I. Ramis-Conde, and M. A. J. Chaplain. Multi-scale mod-
769 elling of the dynamics of cell colonies: insights into cell-adhesion forces and
770 cancer invasion from in silico simulations. J R Soc Interface, 12:20141080,
771 2015.

- 772 [95] H. Hertz. Ueber die berührung fester elastischer körper (on the contact
773 of elastic solids). J Reine Angew Mat, 92:156–171, 1882.
- 774 [96] J. Galle, M. Loeffler, and D. Drasdo. Modeling the effect of deregulated
775 proliferation and apoptosis on the growth dynamics of epithelial cell pop-
776 ulations in vitro. Biophys J, 88(1):62–75, 2005.
- 777 [97] D. Drasdo and S. Hoehme. A single-cell-based model of tumor growth in
778 vitro: monolayers and spheroids. Phys Biol, 2:133–47, 2005.
- 779 [98] D. Drasdo, S. Hoehme, and M. Block. On the role of physics in the growth
780 and pattern formation of multicellular systems: What can we learn from
781 individual-cell based models? J Statist Phys, 128:287–345, 2007.
- 782 [99] K. L. Johnson, K. Kendall, and A. Roberts. Surface energy and the contact
783 of elastic solids. Proceedings of the Royal Society of London. Series A,
784 Mathematical and Physical Sciences, 324(1558):301–313, 1971.
- 785 [100] W. H. Goldmann. Mechanotransduction and focal adhesions. Cell Biol
786 Int, 36(7):649–652, 2012.
- 787 [101] J. Hood and D. Cheresch. Role of integrins in cell invasion and migration.
788 Nat Rev Cancer, 2:91–100, 2002.
- 789 [102] M. W. Pickup, J. K. Mouw, and V. M. Weaver. The extracellular matrix
790 modulates the hallmarks of cancer. EMBO Rep, 15:1243–1253, 2014.
- 791 [103] A. Nagelkerke, J. Bussink, A. E. Rowan, and P. N. Span. The mechanical
792 microenvironment in cancer: How physics affects tumours. Semin Cancer
793 Biol, 35:62–70, 2015.
- 794 [104] K. R. Levental, H. Yu, L. Kass, J. N. Lakins, M. Egeblad, J. T. Erler,
795 S. F. Fong, K. Csiszar, A. Giaccia, W. Weninger, M. Yamauchi, D. L.
796 Gasser, and V. M. Weaver. Matrix crosslinking forces tumor progression
797 by enhancing integrin signaling. Cell, 139(5):891–906, 2009.
- 798 [105] P. P. Provenzano, D. R. Inman, K. W. Eliceiri, and P. J. Keely. Matrix
799 density-induced mechanoregulation of breast cell phenotype, signaling and
800 gene expression through a fak-erk linkage. Oncogene, 28(49):4326–4343,
801 2009.
- 802 [106] P. Friedl and K. Wolf. Plasticity of cell migration: a multiscale tuning
803 model. J Cell Biol, 188:11–19, 2010.
- 804 [107] J. C. Dallon, J. A. Sherratt, and P. K. Maini. Mathematical modelling of
805 extracellular matrix dynamics using discrete cells: fiber orientation and
806 tissue regeneration. J Theor Biol, 199:449–471, 1999.
- 807 [108] R. Shuttleworth and D. Trucu. Multiscale modelling of fibres dynamics
808 and cell adhesion within moving boundary cancer invasion. Bull Math
809 Biol, 81:2176–2219, 2019.

- 810 [109] G. D’Antonio, P. Macklin, and L. Preziosi. An agent-based model for
811 elasto-plastic mechanical interactions between cells, basement membrane
812 and extracellular matrix. Math Biosci Eng, 10(1):75–101, 2013.
- 813 [110] S. P. Chiang, R. M. Cabrera, and J. E. Segall. Tumor cell intravasation.
814 Am J Physiol Cell Physiol, 311(1):C1–C14, 2016.
- 815 [111] M. V. Zavyalova, E. V. Denisov, L. A. Tashireva, O. E. Savelieva, E. V.
816 Kaigorodova, N. V. Krakhmal, and V. M. Perelmuter. Intravasation as a
817 key step in cancer metastasis. Biochemistry (Mosc), 84(7):762–772, 2019.
- 818 [112] L. Zhang, G. Huang, X. Li, Y. Zhang, Y. Jiang, J. Shen, J. Liu, Q. Wang,
819 J. Zhu, X. Feng, J. Dong, and C. Qian. Hypoxia induces epithelial-
820 mesenchymal transition via activation of snail by hypoxia-inducible factor
821 -1α in hepatocellular carcinoma. BMC Cancer, 13:108, 2013.
- 822 [113] L. C. Franssen, T. Lorenzi, A. F. Burgess, and M. A. J. Chaplain. A
823 mathematical framework for modelling the metastatic spread of cancer.
824 Bull Math Biol, 81(6):1965–2010, 2019.
- 825 [114] S. R. McDougall, A. R. Anderson, M. A. J. Chaplain, and J. A. Sherratt.
826 Mathematical modelling of flow through vascular networks: implications
827 for tumour-induced angiogenesis and chemotherapy strategies. Bull Math
828 Biol, 64:673–702, 2002.
- 829 [115] S. R. McDougall, A. R. Anderson, and M. A. J. Chaplain. Mathematical
830 modelling of dynamic adaptive tumour-induced angiogenesis: clinical im-
831 plications and therapeutic targeting strategies. J Theor Biol, 241:564–589,
832 2006.
- 833 [116] M. J. Machado, M. G. Watson, A. H. Devlin, M. A. J. Chaplain, S. R.
834 McDougall, and C. A. Mitchell. Dynamics of angiogenesis during wound
835 healing: a coupled in vivo and in silico study. Microcirculation, 8:183–197,
836 2011.
- 837 [117] M. G. Watson, S. R. McDougall, M. A. J. Chaplain, A. H. Devlin, and
838 C. A. Mitchell. Dynamics of angiogenesis during murine retinal develop-
839 ment: a coupled in vivo and in silico study. J. R. Soc. Interface, 9:2351–
840 2364, 2011.
- 841 [118] A. Boujelben, M. G. Watson, S. R. McDougall, Y.-F. Yen, E. R. Gerstner,
842 C. Catana, T. Deisboeck, T. T. Batchelor, D. Boas, B. Rosen, J. Kalpathy-
843 Cramer, and M. A. J. Chaplain. Multimodality imaging and mathematical
844 modelling of drug delivery to glioblastomas. Interface Focus, 6:20160039,
845 2016.
- 846 [119] D. Drasdo, R. Kree, and J. McCaskill. Monte-carlo approach to tissue-cell
847 populations. Phys Rev E, 52(6):6635–6657, 1995.

- 848 [120] J. Galle, G. Aust, G. Schaller, T. Beyer, and D. Drasdo. Individual cell-
849 based models of the spatial-temporal organization of multicellular systems
850 - achievements and limitations. Cytom Part A, 69:704–10, 2006.
- 851 [121] P. Van Liedekerke, A. Buttenschön, and D. Drasdo. Off-lattice agent-
852 based models for cell and tumor growth: numerical methods, implement-
853 ation, and applications. In M. Cerrolaza, S. Shefelbine, and D. Garzón-
854 Alvarado, editors, Numerical methods and advanced simulation in
855 biomechanics and biological processes, pages 245–267. London, UK; San
856 Diego, CA; Cambridge, MA; Oxford, UK: Elsevier Academic Press, 2018.
- 857 [122] G. Schaller and M. Meyer-Hermann. Multicellular tumor spheroid in an
858 off-lattice voronoi-delaunay cell model. Phys Rev E, 71:051910, 2019.
- 859 [123] J. Galle, D. Sittig, I. Hanisch, M. Wobus, E. Wandel, M. Loeffler, and
860 G. Aust. Individual cell-based models of tumor-environment interactions:
861 Multiple effects of cd97 on tumor invasion. Am J Pathol, 169(5):1802–
862 1811, 2006.
- 863 [124] M. Cytowski and Z. Szymańska. Large scale parallel simulations of 3-d
864 cell colony dynamics. IEEE Comput Sci Eng, 16(5):86–95, 2014.
- 865 [125] M. Cytowski and Z. Szymańska. Enabling large scale individual-
866 based modelling through high performance computing. In ITM Web of
867 Conferences, volume 5, page 00014, 2015.
- 868 [126] M. Cytowski and Z. Szymańska. Large scale parallel simulations of 3-d
869 cell colony dynamics. ii. coupling with continuous description of cellular
870 environment. Comput Sci Eng, 17:44–48, 2015.
- 871 [127] P. Macklin and M. E. Edgerton. Agent-based cell modeling: applic-
872 ation to breast cancer. In V. Cristini and J. S. Lowengrub, edit-
873 ors, Multiscale modeling of cancer: an integrated experimental and
874 mathematical modeling approach, pages 206–234. Cambridge University
875 Press, Cambridge, UK, 2010.
- 876 [128] P. Macklin, M. E. Edgerton, A. Thompson, and V. Cristini. Patient-
877 calibrated agent-based modelling of ductal carcinoma in situ (dcis): from
878 microscopic measurements to macroscopic predictions of clinical progres-
879 sion. J Theor Biol, 301:122–170, 2012.
- 880 [129] P. Macklin, S. Mumenthaler, and J. Lowengrub. Modeling multiscale
881 necrotic and calcified tissue biomechanics in cancer patients: application
882 to ductal carcinoma in situ (dcis). In Multiscale Computer Modeling
883 in Biomechanics and Biomedical Engineering. Studies in Mechanobiology,
884 Tissue Engineering and Biomaterials, volume 14, pages 349–380. Springer,
885 Berlin, Heidelberg, 2013.

- 886 [130] A. Ghaffarizadeh, R. Heiland, S. H. Friedman, S. M. Mumenthaler, and
887 P. Macklin. Physicell: An open source physics-based cell simulator for 3-d
888 multicellular systems. PLoS Comput Biol, 14(2):e1005991, 2018.
- 889 [131] F. Pappalardo, S. Musumeci, and S. Motta. Modeling immune system
890 control of atherogenesis. Bioinformatics, 24:1715–1721, 2008.
- 891 [132] W.-Y. Hu, W.-R. Zhong, F.-H. Wang, L. Li, and Y.-Z. Shao. In silico syn-
892 ergism and antagonism of an anti-tumour system intervened by coupling
893 immunotherapy and chemotherapy: a mathematical modelling approach.
894 Bull Math Biol, 74(2):434–452, 2012.
- 895 [133] J. N. Kather, J. Poleszczuk, M. Suarez-Carmona, J. Krisam, P. Char-
896 oentong, N. A. Valous, C. A. Weis, L. Tavernar, F. Leiss, E. Herpel,
897 F. Klupp, A. Ulrich, M. Schneider, A. Marx, D. Jäger, and N. Halama.
898 In silico modeling of immunotherapy and stroma-targeting therapies in
899 human colorectal cancer. Cancer Res, 77(22):6442–6452, 2017.
- 900 [134] F. R. Macfarlane, T. Lorenzi, and M. A. J. Chaplain. Modelling the
901 immune response to cancer: an individual-based approach accounting for
902 the difference in movement between inactive and activated t cells. Bull
903 Math Biol, 80:1539–1562, 2018.
- 904 [135] R. A. Gatenby and E. T. Gawlinski. A reaction-diffusion model of cancer
905 invasion. Cancer Res., 56:5745–5753, 1996.
- 906 [136] A. J. Perumpanani, J. A. Sherratt, J. Norbury, and H. M. Byrne. Bio-
907 logical inferences from a mathematical model for malignant invasion.
908 Invasion Metastasis, 16:209–221, 1996.
- 909 [137] J. A. Sherratt and M. A. J. Chaplain. A new mathematical model for
910 avascular tumour growth. J Math Biol, 43:291–312, 2001.
- 911 [138] A. Gerisch and M. A. J. Chaplain. Mathematical modelling of cancer cell
912 invasion of tissue: Local and non-local models and the effect of adhesion.
913 J Theor Biol, 505(4):684–704, 2008.
- 914 [139] N. A. M. Monk. Oscillatory expression of *hes1*, *p53*, and *nf- κ b* driven by
915 transcriptional time delays. Curr Biol, 13:1409–1413, 2003.
- 916 [140] M. Sturrock, A. J. Terry, D. P. Xirodimas, A. M. Thompson, and M. A. J.
917 Chaplain. Spatio-temporal modelling of the *hes1* and *p53*-*mdm2* intracel-
918 lular signalling pathways. J Theor Biol, 273:15–31, 2011.
- 919 [141] J. Eliaš, L. Dimitrio, J. Clairambault, and R. Natalini. Modelling *p53*
920 dynamics in single cells: physiologically based ode and reaction-diffusion
921 pde models. Phys Biol, 11:045001, 2014.
- 922 [142] R. Rockne, E. C. Jr Alvord, J. K. Rockhill, and K. R. Swanson. A math-
923 ematical model for brain tumor response to radiation therapy. J Math
924 Biol, 58(4-5):561–578, 2009.

- 925 [143] D. Wodarz. Computational modeling approaches to studying the dynam-
926 ics of oncolytic viruses. Math Biosci Eng, 10(3):939–957, 2013.
- 927 [144] H. Enderling, J. C. L. Alfonso, E. Moros, J. J. Caudell, and L. B. Harrison.
928 Integrating mathematical modeling into the roadmap for personalized ad-
929 aptive radiation therapy. Trends Cancer, 5(8):467–474, 2019.
- 930 [145] A. L. Jenner, F. Frascoli, A. C. F. Coster, and P. S. Kim. Enhancing
931 oncolytic virotherapy: Observations from a voronoi cell-based model. J
932 Theor Biol, 485:110052, 2020.